INVESTIGATION OF PARTICLE MOTION IN THE IMPINGEMENT ZONE OF SWIRLING JETS

P. S. Kuts, É. G. Tutova, N. N. Grinchik, and V. A. Zavadskii

UDC 532.529.5

A solution is obtained for the problem permitting determination of the depth of penetration and angle of deceleration of particles in the impingement zone of swirled jets.

The motion of dispersed particles in vortex spraying apparatuses with impinging streams is very complex and governed by the effect of many forces.

Particle motion in the jet impingement zone has been investigated in [1] for the simplest one-dimensional case. The process can be represented as follows for apparatuses with swirling jet motion. Two oppositely swirling gas-suspension streams move toward each other at an identical velocity. The flow is symmetric relative to both the horizontal channel axis and the plane of jet impingement. Let us consider the case of jet escape into free space and potential flow. For low values of the particle concentration in the stream, the particle interaction and influence on the velocity profile can be neglected. To analyze the hydrodynamics of jet impingement it is possible to limit oneself to an examination of the motion of individual particles. The particle shape is spherical, and we neglect gravitational forces.

As is known, a solid particle experiences multiple damped vibrational displacements in the stream collision zone during jet impingement. Let us determine the maximum depth of particle penetration into the impinging jet and the maximum deviation of the trajectory in the tangential direction.

For a single particle moving at the velocity $\mathbf{W}$ in a gas stream moving at the velocity $\mathbf{W}_g$, the equation of motion can be written as follows:

$$-m\frac{d\mathbf{W}}{d\tau}=\frac{c\gamma_g F}{2}|\mathbf{W}_g+\mathbf{W}|(\mathbf{W}_g+\mathbf{W}). \tag{1}$$

Let us introduce the notation

$$K=\frac{c}{2m}\gamma_g F. \tag{2}$$

Then in cylindrical coordinates (1) is represented as

$$\begin{aligned}
-\frac{\partial W_r}{\partial\tau}&=W_r\frac{\partial W_r}{\partial r}+\frac{W_\varphi}{r}\cdot\frac{\partial W_r}{\partial\varphi}-\frac{W_\varphi^2}{r}+W_z\frac{\partial W_z}{\partial z}+K|\mathbf{W}_g+\mathbf{W}|(W_{gr}-W_r),\\
-\frac{\partial W_\varphi}{\partial\tau}&=W_r\frac{\partial W_\varphi}{\partial r}+\frac{W_\varphi}{r}\cdot\frac{\partial W_\varphi}{\partial\varphi}+\frac{W_r W_\varphi}{r}+W_z\frac{\partial W_\varphi}{\partial\varphi}+K|\mathbf{W}_g+\mathbf{W}|(W_{g\varphi}+W_\varphi),\\
-\frac{\partial W_z}{\partial\tau}&=W_r\frac{\partial W_z}{\partial r}+\frac{W_\varphi}{r}\cdot\frac{\partial W_z}{\partial\varphi}+W_z\frac{\partial W_z}{\partial z}+K|\mathbf{W}_g+\mathbf{W}|(W_{gz}+W_g).
\end{aligned} \tag{3}$$

Going over to total differentials, we obtain the following system of differential equations:

$$\begin{aligned}
-\frac{dW_r}{dr}&=-\frac{W_\varphi^2}{W_r r}+K\frac{|\mathbf{W}_g+\mathbf{W}|(W_{gr}-W_r)}{W_r},\\
-\frac{dW_\varphi}{d\varphi}&=W_r+K\frac{|\mathbf{W}_g+\mathbf{W}|(W_{g\varphi}+W_\varphi)r}{W_\varphi},
\end{aligned} \tag{4}$$

Institute of Heat and Mass Transfer, Academy of Sciences of the Belorussian SSR, Minsk. Translated from Inzhenerno-Fizicheskii Zhurnal, Vol. 30, No. 2, pp. 228-234, February, 1976. Original article submitted February 12, 1975.

$$-\frac{dW_z}{dz} = K\frac{|\mathbf{W}_g + \mathbf{W}|(W_{gz} + W_z)}{W_z}.$$

The Stokes mode domain ($10^{-3} < \mathrm{Re} < 1.0$), for which $c = 24/\mathrm{Re}$ and the transition domain ($10 < \mathrm{Re} < 10^3$) with $c = 12.5/\sqrt{\mathrm{Re}}$ are of greatest interest for our investigations. The Stokes domain is

$$c = \frac{24}{\mathrm{Re}} = \frac{24\nu_g}{|\mathbf{W}_g + \mathbf{W}|d}, \tag{5}$$

from which by substituting (2) and (5) into (4) we obtain

$$K = 24 \cdot 0{,}75\,\frac{\gamma_g \nu_g}{d_p^2 \gamma_p}. \tag{6}$$

Taking account of (5), we write the system (4) as

$$\begin{aligned} -\frac{dW_r}{dr} &= -\frac{W_\varphi}{W_r r} + K\frac{(W_g - W_r)}{W_r}, \\ -\frac{dW_\varphi}{d\varphi} &= W_r + K\frac{(W_{g\varphi} + W_\varphi)}{W_\varphi} r, \\ -\frac{dW_z}{dz} &= K\frac{(W_{gz} + W_z)}{W_z}. \end{aligned} \tag{7}$$

It has been shown in [2] that the theory of jet impact on a wall [3] can be used for symmetric jets.

Then the expression for the velocity potential can be written as follows in the axisymmetric case:

$$\Phi = -\frac{M}{2}(-2z^2 + r^2), \tag{8}$$

where $M = |W_{gl}|/2H$ and W_{gl} is the velocity at the exit from the chamber.

Differentiating (8) with respect to r and z, we obtain an expression for the radial and axial velocity components:

$$W_{gr} = Mr, \quad W_{gz} = -2Mz. \tag{9}$$

Considering particle deceleration in the radial direction insignificant, let us determine the trajectory of its motion. Since $W_{gr} = dr/d\tau$, from (9) we have

$$-\frac{dr}{r} = Md\tau. \tag{10}$$

Integrating (10) we obtain

$$r = r_0 e^{M\tau}. \tag{11}$$

Let us consider the velocities of both gas jets to be zero in the plane of their impingement. The particle velocity in this plane equals the velocity of the lifting gas stream W_{gl} at the exit from the chamber because of inertia and it equals zero at the maximum depth of penetration in the impinging stream [1]. Taking the above into account, the first equation in (7) is not examined, since the law of particle motion (11) is known in the radial direction. Then (7) can be written as

$$-\frac{dW_\varphi}{d\varphi} = Mr + K\frac{(W_{g\varphi} + W_\varphi)r}{W_\varphi}, \tag{12}$$

$$-\frac{dW_z}{dz} = K\frac{(W_{gz} + W_z)}{W_z}. \tag{13}$$

Integrating (12) and (13), we obtain an expression for the magnitude of the maximum deceleration angle and the depth of particle penetration into the impinging stream (axial spatter) for the Stokes domain

$$\varphi_{max} = -\frac{1}{r}\int_{W_{g\varphi}}^{0}\frac{dW_\varphi}{\left[M + \frac{K}{W_{g\varphi}}(W_{g\varphi} + W_\varphi)\right]} = -\frac{W_{g\varphi}}{r(M+K)^2}\left[K\ln\left(\frac{2K+M}{K}\right) - (M+K)\right]; \tag{14}$$

$$z_{max} = 0{,}0166\,\frac{d^2\gamma_p W_{gz}}{\nu_g \gamma_g}. \tag{15}$$

The transition domain for which

$$c = \frac{12{,}5\sqrt{\nu}}{\sqrt{|\mathbf{W}_g + \mathbf{W}|d_p}}, \tag{16}$$

is then

$$K_t = 9.4 \frac{\nu_g^{0.5} \gamma_g}{d_p^{1.5} \gamma_p} . \quad (17)$$

Since $dS_\varphi = rd\varphi$, let us write the system of equations (4) as follows:

$$-\frac{dW_\varphi}{dS_\varphi} = M + K_t [(W_{g\varphi} + W_\varphi)^2 + (W_{gz} + W_z)]^{1/4} \frac{(W_{g\varphi} + W_\varphi)}{W_\varphi} , \quad (18)$$

$$-\frac{dW_z}{dz} = K_t [(W_{g\varphi} + W_\varphi)^2 + (W_{gz} + W_z)]^{1/4} \frac{(W_{gz} + W_z)}{W_z} . \quad (19)$$

Let us express the relationship between the tangential and axial gas stream components as the dependence

$$W_{g\varphi} = \alpha W_{gz},$$

where α is a constant for this radius. Since particle deceleration in the radial direction is not taken into account, we can set $M = 0$.

Taking the above into account, (18) and (19) are written as

$$-\frac{dW_\varphi}{dS_\varphi} = K_t \left(\frac{\alpha^2 + 1}{\alpha^2}\right)^{1/4} \frac{(W_{g\varphi} + W_\varphi)^{3/2}}{W_\varphi} , \quad (20)$$

$$-\frac{dW_z}{dz} = K_t (\alpha^2 + 1)^{1/4} \frac{(W_{gz} + W_z)^{3/2}}{W_z} . \quad (21)$$

Integrating (20) and (21), we obtain an expression for the maximum deceleration path in the tangential and axial directions, respectively,

$$S_\varphi = -\frac{1}{K_t} \left(\frac{\alpha^2}{\alpha^2 + 1}\right)^{1/4} \int_{W_{g\varphi}}^{0} \frac{W_\varphi dW_\varphi}{(W_{g\varphi} + W_\varphi)^{3/2}} = \frac{0{,}23}{K_t} \left(\frac{\alpha^2}{\alpha^2 + 1}\right)^{1/4} \sqrt{W_{g\varphi}} , \quad (22)$$

$$z_{max} = \frac{0{,}23 (\alpha^2 + 1)^{-1/4} \sqrt{W_{gz}}}{K_t} . \quad (23)$$

The time of complete particle deceleration can be found from (20) and (21),

$$\tau_{max} = 0{,}58 \frac{1}{K_t} \left(\frac{1}{\alpha^2 + 1}\right)^{1/4} \frac{1}{\sqrt{W_{gz}}} , \quad (24)$$

Then the expressions for the maximum deceleration angle and the axial spatter are written as follows:

$$\varphi_{max} = 0{,}0245 \frac{1}{r} \frac{d^{1.5} \gamma_r}{\nu^{0.5} \gamma_g} \left(\frac{\alpha^2}{\alpha^2 + 1}\right)^{1/4} \sqrt{W_{g\varphi}} , \quad (25)$$

$$z_{max} = 0{,}245 \frac{d^{1.5} \gamma_r \sqrt{W_g}}{\nu^{0.5} \gamma_g (\alpha^2 + 1)^{1/4}} . \quad (26)$$

The dependences (25) and (26) have been obtained under a number of assumptions whose legitimacy must be verified experimentally.

A method which permits determination of the fluid particle-motion velocity in a swirling gas stream by recording the instant of a change in electrical conductivity of the transducer sensors when they are wetted by the dispersed fluid was used for the investigation.

The practical realization of the method we developed is represented in Fig. 1. The main elements of the measuring circuit are transducers which are connected through autonomous transistorized switches to a recorder: either an N-700 light-beam oscillograph or a ChZ-33 electronic frequency meter. In this case, the latter can operate in the mode to measure time intervals between two electrical signals.

The transducer sensors 7 are fabricated from ϕ 50-100 μ nickel wire with surface lacquer insulation. The wire is wound on a cylinder in two parallel, closely packed windings, whereupon two mutually insulated loops are formed. The outer surface of the loops has the insulation removed and the transducer surface therefore has an open electrical contact with the suspended stream drops. Two leads, one from each transducer loop, are inserted in the autonomous transistorized switch circuit 8, whose output is coupled to the input channel of the recorder 9.

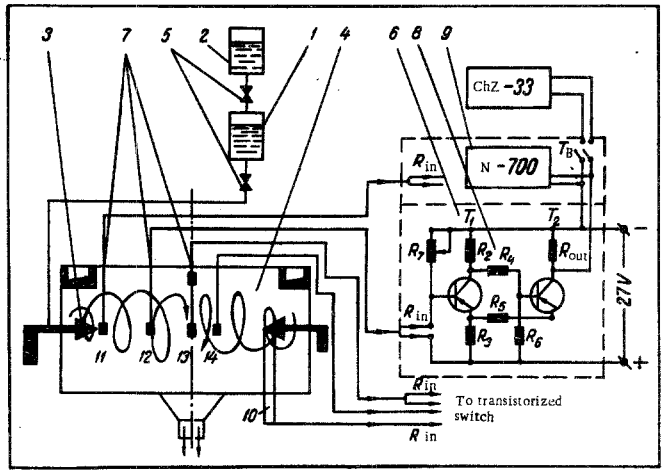

Fig. 1. Diagram of the experimental apparatus [1, 2) tanks for the fluid; 4) vortex chamber; 5) valve; 6) transistorized switch module; see text for remaining notation].

To fix the initial instant at which the fluid emerges from the nozzle, two electrodes 10 of $\phi 50$-μ platinum wire are mounted at the atomizer nozzle exit 3. The electrodes 10 are connected into the measuring circuit of the device 9 analogously to the transducer connection. The threshold of trigger activation was regulated by the resistors R_1 and R_3 for definite values of R_{in} which is interrelated to the electrical resistivity of the drops shorting two adjacent turns of the transducers 7 at the time they are wetted by the fluid. Therefore, the circuit response is determined by the parameters of the resistors R_1, R_3, and the circuit input resistance R_{in} due to the electrical conductivity of the wetting fluid.

The system was checked out with distilled water, hence switching of the transistors T_1 and T_2 did not occur. Then a specific quantity of hydrochloric acid was supplied to the distillate. The electrical resistivity of the water was reduced considerably. The drop in resistance R_{in} results in a voltage appearing at the base of the transistor T_2 which is sufficient to open it. The time of switching of the transistors T_1 and T_2 was fixed by the N-700 recorder, and this uniquely determined the time the liquid phase reached the transducers (the points 11, 12, 13, and 14).

The time intervals between transistor-switch activation, which uniquely determine the time the dispersed liquid phase passes the axial section of the chamber of interest to us, can be determined by means of the oscillograms of the motion velocity.

An oscillogram recording the drop motion in the chamber is shown in Fig. 2. The break in the solid line a shows the time of fluid emergence from the atomizer, and the lines b, c, and d show the time of drop contact with the surface of the transducers mounted at specific distances from the atomizer.

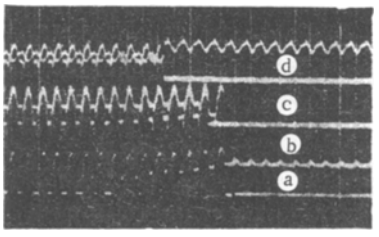

Fig. 2

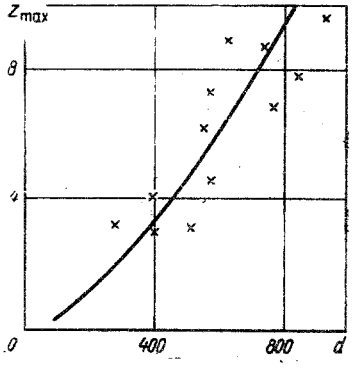

Fig. 3

Fig. 2. Oscillogram recording drop contact with transducers.

Fig. 3. Dependence of the depth of particle penetration in the stream impingement zone on their diameter z_{max}, m; d, μ.

An analysis of the oscillogram shows that distinct deviations of the light beam are observed at the same measurement point. This is evidently caused by the distinct resistance of the drops wetting the transducer.

In turn, the resistance depends on the diameter of the drops. Hence, the size of the drops incident on the transducer can be determined by means of the magnitude of the current.

Experiments conducted with a given different particle diameter, obtained by using a drop generator [4], afforded the possibility of constructing a calibration curve to determine the drop diameter as a function of the value of the current. Results of an analytical computation are compared in Fig. 3 with experimental results characterizing the depth of fluid particle penetration z_{max} in the symmetric domain of the jet impingement zone or, in other words, the particle deceleration path in the axial direction, in order to analyze the hydrodynamics of the swirling jet impingement zone.

The results of an analytical investigation are verified completely satisfactorily by the experimental check.

The maximum value of the deceleration path fluctuated within the range 0.01-0.11 m for fluid drops of the size 100-1000 μ.

NOTATION

m, particle mass; γ_r, specific gravity of the gas; γ_p, specific gravity of the particle; F, middle section; c, frontal drag coefficient; Re, Reynolds number; ν, kinematic viscosity; d, particle diameter; W_{gl}, velocity at chamber exit; H, spacing between end faces; W_φ, W_r, W_z, tangential, radial, and axial gas velocities; τ, time; z_{max}, maximum depth of particle penetration in the swirling impinging stream.

LITERATURE CITED

1. Yu. P. Enyakin, Inzh.-Fiz. Zh., 14, No. 6 (1968).
2. I. T. El'perin, Transport Processes in Impinging Jets [in Russian], Nauka i Tekhnika, Minsk (1972).
3. Bai Shi-I, Theory of Jets [in Russian], Fizmatgiz (1960).
4. E. K. Dabora, Instruments for Scientific Investigations [Russian translation], Mir, Moscow (1967).

BEHAVIOR OF POLYDISPERSE PARTICLE CLOUD IN GAS FLOW AT LOW REYNOLDS NUMBERS

V. M. Liventsov and A. E. Mozol'kov

UDC 532.529.5

Expressions which describe the behavior of particles in a fluidized bed are obtained and studied. Comparative values are given for mass flow and energy of entrained particles as a function of relative concentration of particles of a different type.

A theoretical expression was obtained [1] with the help of a point-force approximation for the resistive force acting on a uniform polydisperse cloud of particles in the direction of gas flow at low Reynolds numbers.

The essence of the point-force approximation is the following: The perturbation introduced by a sphere in a flow at low Reynolds numbers is replaced by a point force applied to the center of the sphere. This force is assumed equal in magnitude but opposite in direction to the viscous force acting on a particle in the direction of flow.

All-Union Scientific-Research and Planning Institute of the Oil-Processing and Petrochemical Industries, Moscow. Translated from Inzhenerno-Fizicheskii Zhurnal, Vol. 30, No. 2, pp. 235-239, February, 1976. Original article submitted September 11, 1974.